Journal of Engineering and Sustainable Development
Vol. 29, No. 06, November 2025
https://jeasd.uomustansiriyah.edu.iq/index.php/jeasd
ISSN 2520-0917
Research Article
https://doi.org/10.31272/jeasd.3013

Advanced Groundwater Quality Assessment Using Geochemical Analysis and Water Quality Indices with Fuzzy Logic

Lakhdar Seraiche[1]*, Messaoud Ghodbane[1], Tahar Selmane[2], Mostafa Dougha[1]

[1]Laboratory of City, Environment, Hydraulics and Sustainable Development, Department of Hydraulic, Faculty of Technology, Mohamed Boudiaf University, University Pole, Road Bordj Bou Arreridj, M'sila 28000, Algeria
[2]Department of Hydraulics and Civil Engineering, University of Ghardaia, 47000, Algeria

*Email: lakhdar.seraiche@univ-msila.dz

Article Info

Received	**21/09/2024**
Revised	**14/05/2025**
Accepted	**14/05/2025**

Abstract

Groundwater resources in the semi-arid region south of Chott Hodna (Algeria) are increasingly threatened by depletion and salinization, threatening both human consumption and agriculture. This study assessed groundwater quality by analyzing the physicochemical parameters of 45 well samples. It used arithmetic, entropy-weighted, and fuzzy logic-based water quality indices (WQI, EWQI, and FWQI), integrated with GIS-based spatial analysis, to address data uncertainties and variability. The results revealed WQI values ranging from 59.51 to 233.68, with 64.44% of the wells classified as having poor quality due to high concentrations of sulfate, chloride, calcium, and nitrate. EWQI and FWQI showed consistent contamination patterns, with FWQI demonstrating greater accuracy by reducing extreme classifications. Spatial analysis highlighted poor water quality in the Maadher agricultural area, while better quality was observed at the eastern and western ends. Challenges included managing data variability, managing complex methodologies, and ensuring reliable spatial interpolation. The ordinary kriging technique with a spherical semivariogram model effectively identified key pollutants, including nitrate (NO_3^-), chloride (Cl^-), and electrical conductivity (EC), concentrated near wadis and agricultural areas.

Keywords: Chott Hodna, Geochemical processes, Groundwater, Water Quality Indices, Spatial Interpolation GIS.

1. Introduction

Groundwater is a vital resource in semi-arid and arid regions, supporting human consumption, agriculture, and industry. However, it is increasingly degraded by natural geochemical processes and anthropogenic activities, but it remains significant. Natural factors such as aquifer mineralogy, weathering mechanisms, and ion exchange reactions considerably influence groundwater composition [1]-[2]. These processes are further aggravated by anthropogenic activities such as bad agricultural practices, improper municipal waste disposal, and wastewater effluents from zones located near wadi banks that carry pollutants such as nitrates, pesticides, and heavy metals into the aquifer [1]. In the southern Chott Hodna of Algeria, these combined actions lead to salinization and contamination of groundwater, endangering both public health and agricultural productivity. The complexity of groundwater quality assessment requires robust methodologies that account for both data variability and uncertainty. Traditional water quality indices (WQIs) are widely used because they simplify the aggregation of physicochemical parameters into a single score, facilitating water quality monitoring and management [3]-[5]. However, these indices often oversimplify complex datasets [1]-[6]. Recent advances, such as the entropy-weighted water quality index (EWQI) and fuzzy logic-based water quality index (FWQI), provide increased accuracy. The EWQI incorporates extended parameter sets and refined weighting factors [7]-[8], while the FWQI uses fuzzy logic systems to handle data uncertainties via probabilistic membership functions [9]-[10]. Together, these indices provide a balanced approach and enhance the water quality assessments for drinking and agricultural purposes.

Geospatial analysis increases groundwater quality assessment by visualizing contamination patterns and identifying areas of poor quality. Geographic information system (GIS) tools combined with interpolation methods such as inverse distance weighting (IDW) and ordinary Kriging (OK) allow detailed spatial analysis of groundwater quality [11]-[13]. These methods incorporate spatial variability and data correlations, enabling reliable predictions and adequate delineation of areas with diverse water quality [13]-[14]. This research provides a comprehensive understanding of groundwater quality by examining the interplay between natural processes and anthropogenic influences.

2. Materials and Methods

A four-phase approach was used to develop the research methodology: laboratory analysis, replication and validation of results, calculation of water quality indices, and finally, generation of spatial distribution maps using ordinary Kriging or IDW (Inverse Distance Weighting). The schematic representation of the study's approach is illustrated in Fig. 1, offering a visual depiction of the sequential flow of activities.

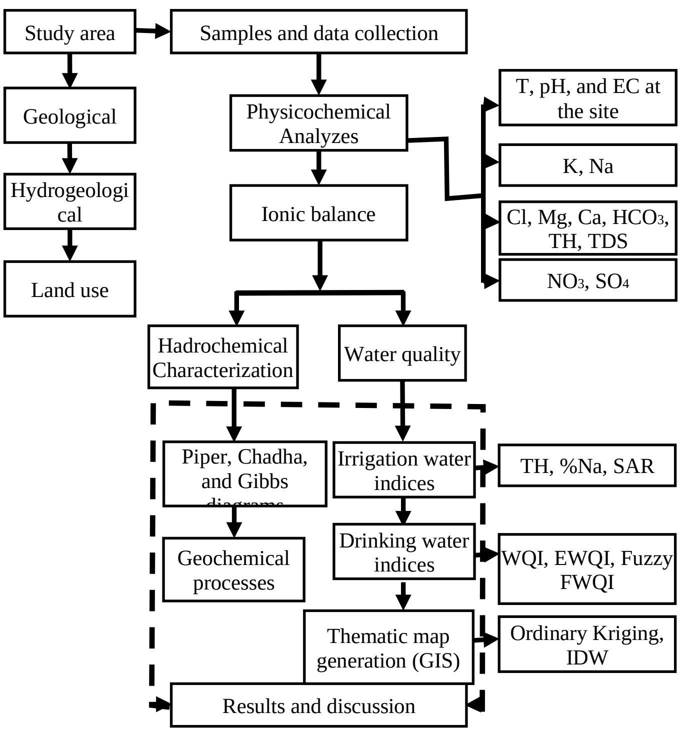

Figure 1. Flowchart of the methodology adopted in this study

2.1. Study Area

The study area, south of the Chott Hodna (Algeria), is in a semi-arid zone, a largely dried-up enclosed lake located in the Hodna basin. The region is blessed with a combination of shallow and deep aquifers that are vital for agricultural and domestic needs. At the same time, the increasing effects of climate change are leading to overexploitation of the aquifers [15]. The South Chott Hodna aquifer serves as the leading water resource essential for domestic use (e.g., drinking) and irrigation needs via pumping from wells. The region faces problems of inadequate availability of groundwater suitable for domestic and agricultural needs, similar to those observed in many countries [16].

The study area encompasses the southern expanse of Chott Hodna within the Hodna basin, situated southeast of the capital, Algiers. Geographically, it spans the coordinates of 4°6' to 4°48' east longitude and 35°7' to 35°28' north longitude, with an average elevation of 450 m above sea level Fig. 2. The terrain is characterized by dunes, recent alluvial deposits, and isolated rocky slopes, fostering wind erosion due to the sandy texture and a lack of natural vegetation cover.

Encompassing approximately 112730 hectares, the study area is demarcated by Chott Hodna to the north, Mount Meharga to the south, Summit Kerdada and Mount Aouidja to the southwest, Mount Baieun and Arar to the west, and M'cif Wadi to the east. The region experiences an arid to semi-arid climate marked by mild, humid winters and hot, dry summers. Low levels characterize rainfall. Hydrographically, the study area includes four main wadis: Bousaada, Roumana, Maîter, and M’cif.

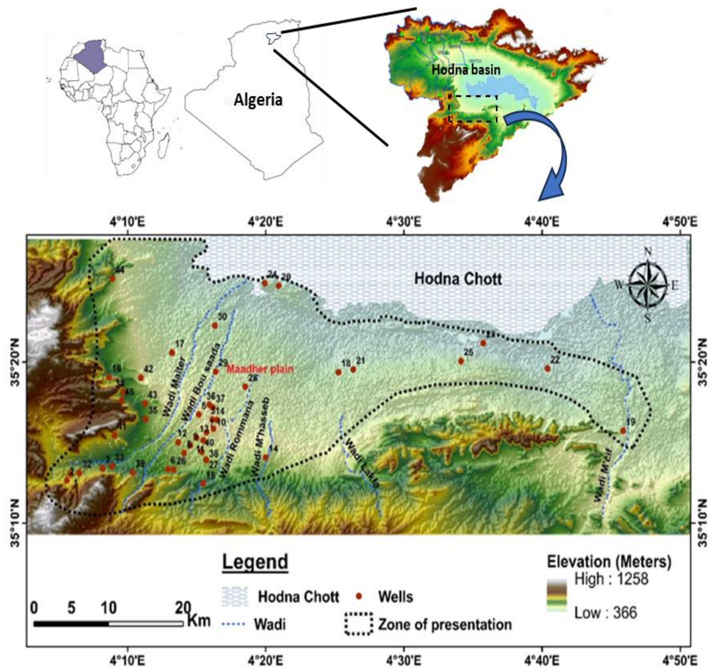

Figure 2. Geographic location, elevation, and well positions in the study area

The first two wadis flow into low-lying areas, while the last two feed the Chott Hodna during floods (Fig. 2). These wadis play a crucial role in replenishing the water table. The region's soils, composed of brown and reddish-brown sandy clays, are suitable for cultivation.

The results of the geological studies shown in Fig. 3 reveal the presence of Triassic formations south of the Hodna Basin Mountains, Cretaceous limestones to the south and west, and Miocene sandstones overlain by Cretaceous formations. The complex Mio-Plio-Quaternary aquifer, with a thickness of almost 250 m in the central part of the plain, plays a key role in the hydrogeology of the region [17]-[18]. This aquifer is characterized by its heterogeneity and anisotropy due to its composition of clays, sandy clays, sandstones, and occasionally sands and clayey conglomerates. The primary aquifers consist of conglomerates and sandy formations from the continental

Mio-Pliocene period, which are connected to Cretaceous formations. Recharge occurs mainly by water infiltration from seasonal wadis.

Furthermore, the interface between phreatic and deep aquifers is imperfect and fractured, allowing significant cross-communication that influences water quality and storage dynamics [19]. Over the last five decades, anthropogenic activities, such as increased groundwater extraction for irrigation, have contributed to a significant decline in groundwater levels, with some areas experiencing a drop exceeding 15 meters since the 1970s [20]. Furthermore, shallow aquifers are vulnerable to contamination due to poor agricultural practices, inadequate well construction, and insufficient aquifer protection measures. Farmers' wells, ranging in depth from 90 to 220 m, often lack adequate isolation between aquifers (based on salinity), further increasing the risk of deep aquifer contamination [19].

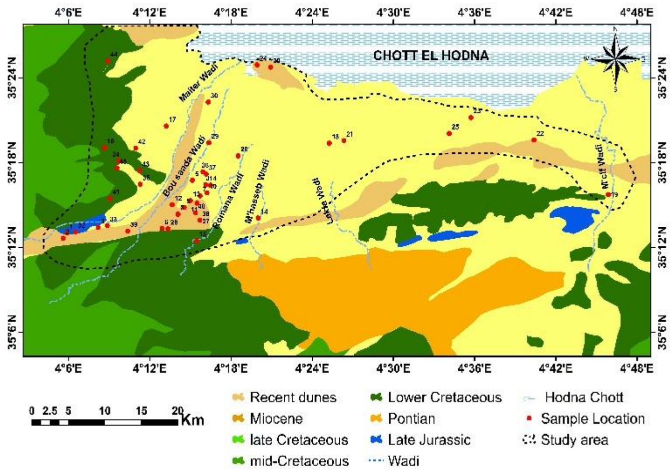

Figure 3. Geological map of the southern Hodna Chott with well locations

2.2. Sampling and Collection

Water samples were collected from farmers' wells in the study area to analyze major anions and cations. The sampling process followed the standardized methodology described in [21], with the campaign conducted from 10 to 25 September 2019. A total of 45 groundwater samples were systematically obtained using clean polyethylene bottles, ensuring consistent collection intervals of 10 to 15 minutes after the start of pumping. To ensure accuracy and reliability, all parametric analyses were performed in duplicate. On the site, the temperature, electrical conductivity (EC), and pH (potential of hydrogen) were quickly measured using the WTW Cond 3110 device. After collection, the samples were quickly transported to the analysis laboratory of the Algerian Company Water Utilities for a more in-depth analysis of the primary ions. Concentrations of calcium (Ca^{2+}), magnesium (Mg^{2+}), bicarbonate (HCO_3^-), and chloride (Cl^-) were determined by volumetric titration. Specifically, Ca^{2+} and Mg^{2+} levels were determined by titration with 0.01 N EDTA solution, while HCO_3^- and Cl^- amounts were measured by methods using HCl and AgNO3, respectively. Sodium (Na^+) and potassium (K^+) amounts were determined using a JENWAY 6850 flame photometer. Sulfates (SO_4^{2-}) and nitrates (NO_3^-) were analyzed by ODYSSEY DR 2500 UV/visible spectrophotometry using calorimetric methods. All parametric analyses were performed twice.

Water physicochemical data were thoroughly analyzed to determine the determining variables of water quality and to generate the corresponding quality indices. Finally, the ordinary kriging technique was used to visually represent the spatial distribution of key ions and quality indices, thus providing meaningful information on groundwater quality throughout the study area.

2.3. Water Drinking Indices

2.3.1. Water quality index (WQI)

For the past few decades, the Water Quality Index (WQI) has been used as an effective tool for ranking water quality for public use. It has been widely used for determining the quality of surface and groundwater [12]-[22]. WQI is a rate-converted indicator that represents water quality according to specific needs. WQI is a composite calculated quantity that reflects the effect of various water quality parameters (variables). WQI has been described as a rapid and systematic model for assessing and ranking water quality parameters [4]. Weights are assigned to the variables, and their outputs are combined to calculate the WQI. The obtained value will then be used to rank the water quality from poor to optimal on a scale ranging from 0 to 100. Observation and monitoring of environmental variables can be carried out using different methodological approaches. A weighted arithmetic water quality index was used in this study. It would be expressed as an equation based on eleven measurable variables from individual samples collected from wells in the field area. The steps to calculate the index are as follows: First, each parameter (pH, EC, TDS (Total Dissolved Solids), Ca^{2+}, Mg^{2+}, HCO_3^-, Cl^-, SO_4^{2-}, NO_3^-, Na^+ and K^+) is given a weight (W_j) ranging from 1 to 5 depending on its importance for the potability assessment; the values for drinking water are presented in Table 1.

Table 1. Weight and relative weight of each parameter used for the WQI calculation

Parameter*	**WHO (2011)**	W_j	**WQI** RW_j	**EWQI** ω_j
pH	6.5-8.5	4	0.125	0.006
EC	1500	3	0.094	0.090
TDS	1000	4	0.125	0.090
Ca^{2+}	75	2	0.063	0.070
Mg^{2+}	100	2	0.063	0.081
HCO_3^-	300	2	0.063	0.137
Cl^-	250	3	0.094	0.095
SO_4^{2-}	250	3	0.094	0.094
NO_3^-	50	5	0.156	0.093
Na+	200	3	0.094	0.136
K+	12	1	0.031	0.109
	$\sum W_j \rightarrow$	32	1.0	1.0

*All parameters are in mg/l except EC (25°C) in µs/cm, T in °C, and pH without unit.

Relative weight (RW_j) of the water quality parameter j was computed using equation (1) [23], where n is the number of parameters.

$$RW_j = \frac{w_j}{\sum_{i=1}^{n} w_j} \tag{1}$$

The quality rating scale for each parameter was calculated by dividing its concentration in each water sample by its respective standards according to WHO (2011) and multiplying the results by 100 [22]-[23].

$$q_j = \frac{c_j}{s_j} \times 100 \tag{2}$$

q_j is the quality rating scale, $and\ C_j$ is the concentration of each chemical parameter j in each sample, measured in mg/l. S_j is the World Health Organization standard for each chemical parameter in mg/l according to the guidelines of the WHO [24]. Then, for deriving the WQI value, the water quality sub-index (SI_j) for each parameter [22]-[23] is calculated using equation (3).

$$SI_j = RW_j \times q_j \tag{3}$$

Finally, the water quality index (WQI) is calculated by using the water quality sub-index (SI_j)

$$WQI = \sum_{j=1}^{n} SI_j \tag{4}$$

WQI results are evaluated into five types of water: excellent Water (WQI < 50), good Water (WQI = 50–100), poor water (WQI = 100–200), very poor water (WQI = 200–300), and water unsuitable for drinking (WQI > 300).

The weighting factors for the quality indices are adjusted to reflect the environmental constraints characteristic of semi-arid regions, ensuring that the index accurately represents water quality concerns [23]-[26].

2.3.2. Entropy-weighted water quality index (EWQI)

The calculation of the EWQI took into account the guidelines provided by the WHO [24]. The EWQI is determined by using an entropy-weighted value. The weight of each parameter is defined by information entropy, which helps reduce the inaccuracy caused by neglecting the weight [27]. In 1948, Shannon proposed the concept of information entropy [9]. Entropy quantifies the level of unpredictability associated with forecasting the result of a probabilistic event. The notion of entropy has been utilized in the domain of water quality [28]. The EWQI calculation involved the implementation of the following procedures [28]: Before any analysis, it is necessary to establish the entropy weight for each quality metric. Pre-processing for data normalization should be employed to mitigate the influence of disparate units.

$$X = \begin{bmatrix} x_{11} & x_{12} & \dots & x_{1n} \\ x_{21} & x_{22} & \dots & x_{2n} \\ \vdots & \vdots & \ddots & \vdots \\ x_{m1} & x_{m2} & \dots & x_{mn} \end{bmatrix} \tag{5}$$

For the efficiency type, the normalization construction function is

$$y_{ij} = \frac{x_{ij} - (x_{ij})_{min}}{(x_{ij})_{max} - (x_{ij})_{min}} \tag{6}$$

x_{ij}: measured value of parameter j for sample i. $(x_{ij})_{max}$: Maximum value of parameter j. $(x_{ij})_{min}$: Minimum value of parameter j. y_{ij}: Normalized value of parameter j for sample i.

After transformation, we can obtain a new matrix of standard quality $[Y]$.

$$Y = \begin{bmatrix} y_{11} & y_{12} & \dots & y_{1n} \\ y_{21} & y_{22} & \dots & y_{2n} \\ \vdots & \vdots & \ddots & \vdots \\ y_{m1} & y_{m2} & \dots & y_{mn} \end{bmatrix} \tag{7}$$

Then the ratio of the index value of parameter j and i the sample is

$$P_{ij} = y_{ij} / \sum_{i=1}^{m} y_{ij} \tag{8}$$

P_{ij}: Probability of parameter j for sample i. The entropy of parameter (e_j) is expressed by the following formula below:

$$e_j = \frac{1}{ln(m)} \sum_{i=1}^{m} P_{ij}\ lnP_{ij} \tag{9}$$

m: Number of samples. $P_{ij}\ lnP_{ij}$: Contribution of parameter j for sample i. The smaller the value of e_j, the greater the effect of the parameter j. Then the normalized entropy weight (ω_j) of parameter j can be calculated with the following formula [27]-[28]:

$$\omega_j = \frac{1 - e_j}{\sum_{j=1}^{n}(1 - e_j)} \tag{10}$$

The next step is to calculate the EWQI, which consists of assigning a quality assessment scale (q_j) to each parameter j. The q_j is obtained by the formula [27]-[28]:

$$q_j = \frac{c_j}{s_j} \times 100 \tag{11}$$

Where C_j is the value in mg/l of each quality parameter for each water sample, S_j is the WHO-recommended standard limit for each parameter in mg/l for drinking water. When the parameter j is exactly equal to its permitted value, the q_j is just above 100, and when it is completely absent from the water, the q_j is 0. The EWQI can be calculated in the last step by the following formula:

$$EWQI = \sum_{j=1}^{n} \omega_j\, q_j \tag{12}$$

According to the EWQI, water samples are classified into five categories, ranging from "excellent water" to "extremely poor water" [28]. The classification of water categories is listed in Table 2.

Table 2. Categories of WQI, EWQI, and FWQI

WQI value	Category	EWQI Value	Category	FWQI Value	Category (SSL)*
<50	Excellent	<50	Excellent	> 80	Excellent
50-100	Good	50 - 100	Good	60 - 80	Good
100-200	Poor	100 - 150	Medium	40 - 60	Moderate
200-300	Very Poor	150 - 200	Poor	20 - 40	Poor
> 300	Unsuitable	> 200	Very poor	≤ 20	Very Poor

* SSL: Standardized Set of Linguistic Labels for FWQI

In both WQI and EWQI, the same weighting factors are employed to represent the relative importance of each water quality parameter (Table 1). These weights ensure that critical parameters are given more weight in the final index score and increase their relevance by considering their expected impact on water quality and human health.

2.3.3. Fuzzy water quality index (FWQI)

The Fuzzy Water Quality Index (FWQI) is a state-of-the-art tool used to assess groundwater quality by integrating multiple parameters into a fuzzy logic framework. FWQI adopts a rather vulgarized fuzzy logic to address the uncertainty and imprecision of water quality data that judiciously represents the degree of membership at each assessment level compared to traditional WQIs [9].

Fuzzy Water Quality Index (FWQI) involves the following steps: Fuzzification, where accurate values of water quality parameters are converted into fuzzy sets using membership functions. Rule-based inference: Defines a set of fuzzy rules to quantify the relative impact of multiple water quality parameters grouped into one. Aggregation: Combines the outputs of all fuzzy rules to generate a fuzzy output. Defuzzification: Converts the fuzzy output into an accurate value, resulting in the final FWQI score [29]-[30].

The FWQI is calculated using fuzzy membership functions for each water quality parameter, which are mapped to a range between 0 and 1. Each parameter is classified into different quality classes based on its concentration levels, represented by the triangular membership function (μ_j), defined as [29]:

$$\mu_j(x;a,b,c) = \begin{cases} 0 & if\ x \le a \\ \frac{x-a}{b-a} & if\ a < x \le b \\ \frac{c-x}{c-b} & if\ b < x < c \\ 0 & if\ x \ge c \end{cases} \tag{13}$$

Where a, b, and c are the parameters defining the triangular shape of the membership function based on WHO limits (2011), representing the minimum acceptable, ideal, and maximum permissible levels for each parameter. x is the value of the parameter. The overall FWQI is derived by aggregating the fuzzy membership values of all parameters using a weighted sum or an average approach, as shown in:

$$FWQI = \frac{\sum_{j=1}^{n} \omega_j . \mu_j}{\sum_{j=1}^{n} \omega_j} \times 100 \tag{14}$$

Where ω_j is the weight of the j parameter, and μ_j is its membership value [31]. Recent studies have demonstrated the efficacy of FWQI in managing water quality assessments in various geographic regions, highlighting its adaptability and precision [32]-[33].

2.4. Water irrigation indices

Irrigation suitability was evaluated by various ionic parameters (mEq/l) and indices, including TH (Total Hardness), %Na (Percent Na), SAR (Sodium Adsorption Ratio) [34]-[35].

$$TH = 2.5 \times Ca^{2+} + 4.1 \times Mg^{2+} \tag{15}$$

$$\%Na = 100 \times \frac{Na^+ + K^+}{Na^+ + K^+ + Mg^{2+} + Ca^{2+}} \tag{16}$$

$$SAR = \frac{Na^+}{\sqrt{\frac{Mg^{2+} + Ca^{2+}}{2}}} \tag{17}$$

2.5. Spatial Interpolation in GIS: Ordinary Kriging or IDW Methods

The section discusses two prominent spatial interpolation techniques used in Geographic Information Systems (GIS): Ordinary Kriging (OK) and Inverse Distance Weighted (IDW) methods. Kriging is based on the principle of spatial autocorrelation between observed data points, where statistical methods are employed to infer what values would be measured at unobserved locations. It uses a semivariogram, which helps to estimate the partial spatial correlation gradient as a function of the geographical distance between sampling points [36]-[37]. Ordinary Kriging offers the Best Linear Unbiased Estimate (BLUE) through the use of spatially dependent variance from the semivariogram, which guarantees a better prediction quality compared to IDW or others [16]. This method uses the variogram to estimate spatial dependence, which improves prediction reliability [28]-[38].

Conversely, the IDW method is a deterministic interpolation approach that calculates unknown values as a linear combination of known values, with their influence decreasing as distance increases [38]. It has a typical distance-weighted power function to weight the contribution of closer points based on their proximity [12]-[13]. IDW is beneficial when data points are uniformly distributed, or in cases where the statistical assumptions required for Kriging and similar, more advanced methods do not hold.

We implemented both methods using ArcGIS software to illustrate how they could be performed on a spatial analysis. The main difference between ordinary Kriging and inverse distance weighting (IDW) approaches is the assumptions about the relationship between points and interpolation. Ordinary Kriging is a geostatistical approach that builds upon spatial autocorrelation theory by modeling spatial dependencies using a semivariogram, which incorporates distance and spatial variance. On the contrary, IWD is a deterministic method that assumes values near unknown points have more influence regardless of spatial correlation, employing a straightforward distance-based weighting function. Although Kriging can be more accurate when spatial variance is modeled, it relies more on statistical assumptions and calculations. In contrast, IDW is a much simpler and more efficient approach for data with a uniform distribution, but it will provide less accuracy if the underlying spatial structure is complex [39].

3. Results and Discussion

3.5. Statistical Description of Groundwater Samples

The accuracy of analytical ion measurement was assessed using absolute ion balance (IB) calculations, which revealed a charge balance inaccuracy of less than 6% for each sample. The majority of sample analyses demonstrated commendable accuracy.

3.5.1. pH and electrical conductivity

In Table 3, the groundwater pH values ranged from 6.60 to 8.15, with an average of 7.43, aligning with WHO standards for drinking water. In contrast, Electrical Conductivity (EC) values spanned from 1033.00 µS/cm to 5980.00 µS/cm, averaging 1937.90 µS/cm. Over 70% of the samples exceeded the recommended threshold of 1500 µS/cm, particularly in wells 05, 06, 12, 13, 14, 16, 17, 34, 36, 41, and 45. These elevated values suggest significant mineral content, indicative of high salinity, potentially linked to both natural geochemical processes and anthropogenic activities.

3.5.2. Cation and anion concentrations

Groundwater analyses revealed elevated concentrations of key cations (Ca^{2+}, Mg^{2+}, Na^{+}, K^{+}) and anions (SO_4^{2-}, Cl^{-}, HCO_3^{-}, NO_3^{-}) compared to WHO guidelines, as shown in Table 3. Calcium and magnesium, derived from water-rock interactions, significantly exceeded permissible levels, contributing to the extreme hardness observed in 93.33% of samples. Sulfate emerged as the dominant anion due to the dissolution of gypsum or anhydrite. At the same time, elevated levels of chloride, bicarbonate, and nitrate highlighted the combined effects of natural processes and anthropogenic pollution, particularly from agriculture and wastewater. The ion concentration trends were ranked as $Ca^{2+} > Na^{+} > Mg^{2+} > K^{+}$ for cations and $SO_4^{2-} > Cl^{-} > HCO_3^{-} > NO_3^{-}$ for anions.

Table 3. Statistical description of the physicochemical results of the samples analyzed

Parameter*	Algerian standard (2011)	WHO standard (2011)	Min	Max	Mean	CV (%)	Sample exceeding WHO standard (%)
T	25	-	12.50	30.50	20.80	24.51	0.00
pH	6.5 - 9.0	6.5 - 8.5	6.60	8.15	7.43	3.94	0.00
EC	2800	1500	1033.00	5980.00	1937.90	42.67	73.33
TDS	1500	1000	668.15	3389.00	1165.55	38.58	64.44
Ca^{2+}	200	75	88.00	544.00	258.43	45.45	100.00
Mg^{2+}	150	100	34.00	214.00	99.30	36.93	46.66
HCO_3^{-}	-	300	102.00	488.00	284.92	34.31	53.33
Cl^{-}	500	250	67.00	902.00	242.08	68.49	35.55
SO_4^{2-}	400	250	200.00	850.00	577.66	28.80	95.55
TH	200	500	460.00	12200.00	1389.53	145.67	93.33
NO_3^{-}	50	50	2.00	262.00	73.85	78.10	57.77
Na^{+}	200	200	27.00	290.00	82.77	56.90	2.22
K^{+}	12	12	1.90	14.80	5.85	44.33	2.22

*All parameters are in mg/l except EC (25°C) in µs/cm, T in °C, and pH without unit.

3.5.3. Statistical analysis and implications

Statistical evaluation underscores significant groundwater quality concerns in the region. High EC and TDS levels in over 70% of samples reflect salinity issues stemming from dissolved salts and anthropogenic contributions. Excessive Ca^{2+} and SO_4^{2-} concentrations correlated with extreme hardness levels unsuitable for domestic use. Nitrate contamination exceeded limits in 57.77% of samples, predominantly due to fertilizer use and waste near wadis. These findings emphasize the interplay between natural geochemical processes and human activities, underscoring the urgent need for sustainable groundwater management strategies.

3.6. Geochemical Processes in Aquifer

The hydrochemical facies concept identifies distinct groundwater families within an aquifer, each exhibiting unique chemical composition, typically involving ions like Ca^{2+}, Mg^{2+}, Cl^{-}, SO_4^{2-}, Na^{+}, K^{+}, HCO_3^{-}, and NO_3^{-} [40]. The Piper diagram (Fig. 4) is employed to classify water samples and reveal trends, showing that all wells have low carbonate concentrations ($CO_3^{2-} + HCO_3^{-} \approx 10\%$) and varying chloride/nitrate levels (10-50%, exceeding 60% in wells 19, 23, and 37). Sulfate ratios average between 30% and 70%. Cation analysis reveals high Ca^{2+} and low Mg^{2+} concentrations across all samples.

The Chadha diagram Fig. 4 complements the Piper diagram by identifying groundwater samples mainly as Ca-Mg-Cl-type, except for well 44, which is Na-Cl-type, indicating reverse ion exchange processes involving Ca^{2+}, Mg^{2+}, and Cl^{-} [35]. Both diagrams consistently categorize the groundwater as SO_4^{2-}-Cl^{-}-Ca^{2+}-Mg^{2+} type, suggesting salinization due to high concentrations of SO_4^{2-}, Cl^{-}, NO_3^{-}, Ca^{2+}, Na^{+}, and Mg^{2+}.

3.7. Identification of Water-Rock Interaction

The Gibbs diagram categorizes groundwater hydrochemistry into three processes: precipitation dominance, rock dominance, and evaporation dominance [41]. Fig. 5 reveals that evaporation is the primary natural process affecting the water chemistry of the studied wells, particularly those near the Chott Hodna, due to significant rock weathering. $Na^{+}/(Na^{+} + Ca_2^{+})$ ratios (ranging from 0.1 to 0.61, with an average of 0.35) confirm considerable cation exchange processes within the aquifer [42].

Fig. 6a shows that most samples are close to the bisector line in the Ca_2^{+} and SO_4^{2-} relationship, indicating a predominance of sulfate (SO_4^{2-}) except for wells 7, 8, 10, 14, 23, and 38, where carbonate precipitates form above the bisector line, suggesting evaporation's role in regulating groundwater composition. Fig.6b highlights that 70% of samples lie above the bisecting line in the Ca_2^{+} and Na^{+} relationship, implying halite dissolution's impact on well salinity, as further supported by Fig. 6c. Finally, Fig. 6d, which depicts the carbonate and silicate-weathering index, shows all samples above the bisector line, indicating a significant influence of carbonate rock on groundwater mineralization.

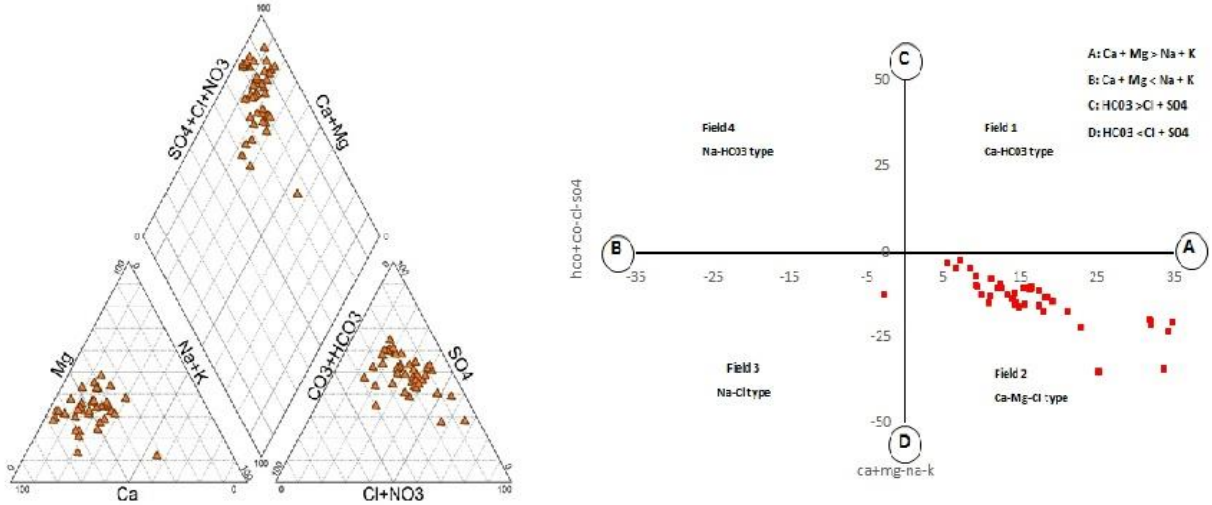

Figure 4. Piper and Chadha diagrams of the groundwater samples

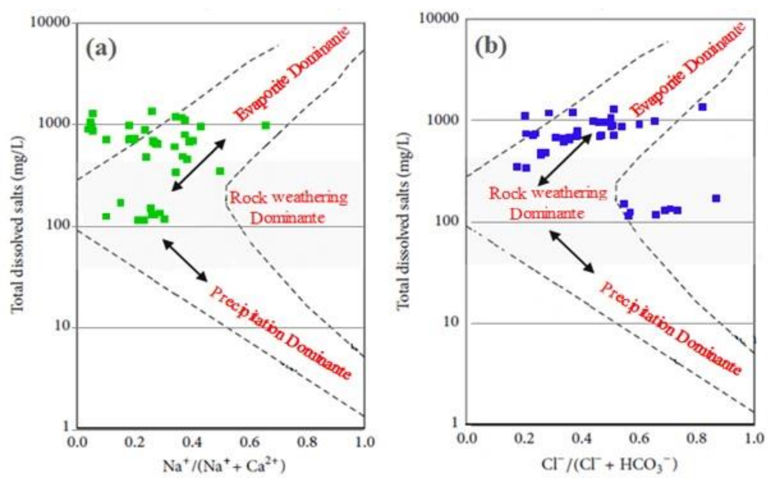

Figure 5. Geochemical controlling mechanism according to Gibbs diagram: (a) TDS vs. $Na^+/(Na^+ + Ca^{2+})$, and (b) TDS vs. $Cl^-/(Cl^- + HCO_3^-)$

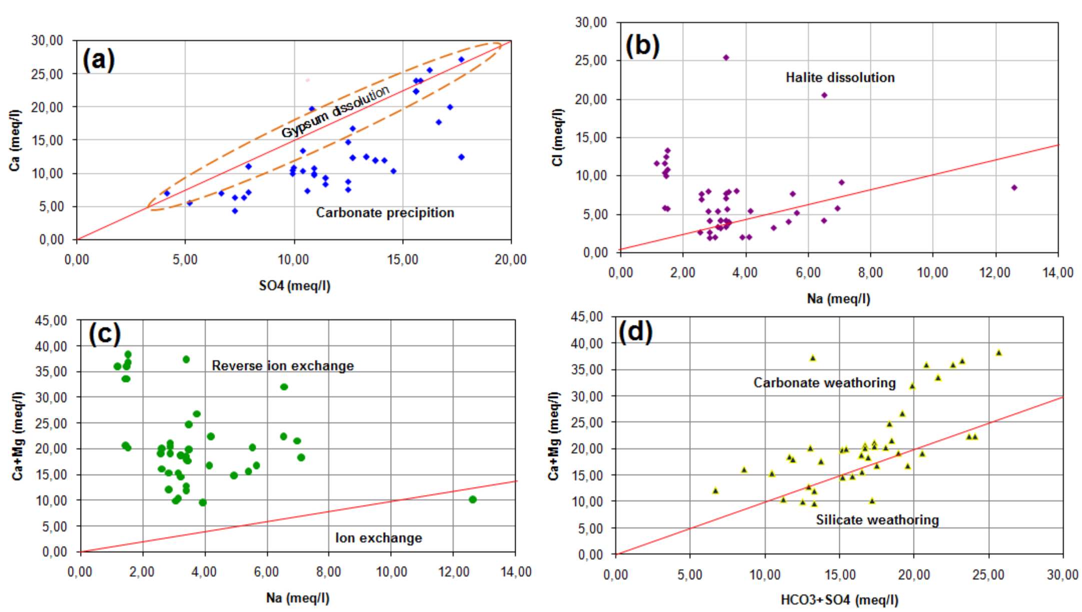

Figure 6. a) Plot of SO_4^{2-} against Ca^{2+} b) Plot of Na^+ against Cl^- c) Plot of Na^+ against $(Ca^{2+} + Mg^{2+})$ d) Plot of $(HCO_3^- + SO_4^{2-})$ against $(Ca^{2+} + Mg^{2+})$

3.8. Assessment of Groundwater for Irrigation and Drinking Using Water Quality Indices

3.8.1. Irrigation purposes

The groundwater samples underwent evaluation for their suitability for irrigation purposes using various indices, and the results are summarized in Table 4. Considering the total hardness (TH) values, 76% of the samples demonstrate soft water quality (TH < 75), with the remaining 24% falling into the moderately hard category. Assessing the Percent Sodium (%Na), 72.72% of the total samples are classified as excellent for irrigation, while 24.24% fall into the good category. Notably, based on the SAR values, it can be concluded that all aquifer samples contain water of exceptional quality, as evidenced by SAR values consistently below 10.

Table 4. Irrigation quality indices of the study area

	Range	Category	Nbr of samples	% of samples
Total Hardness (TH)	<75	Soft	34	75.56%
	75-150	Moderately hard	11	24.44%
	150-300	Hard	-	-
	>300	Very hard	-	-
Percent sodium (%Na)	<20	Excellent	31	68.89 %
	20-40	Good	13	28.89 %
	40-60	Permissible	1	2.22 %
	60-80	Doubtful	-	-
	>80	Unsafe	-	-
Sodium Absorption Ratio (SAR)	<10	Excellent	All samples	100%
	10-18	Good	-	-
	18-26	Doubtful	-	-
	>26	Unsuitable	-	-

3.8.2. Drinking water quality indices

The assessment of groundwater suitability for drinking in the Chott Hodna South region used water quality indices, and the results shown in Fig.7 reveal WQI values ranging from 59.51 to 233.68 across 45 wells. The majority (64.44%) fell into the poor water quality category, with 30.11% classified as good water quality. Notably, wells 10, 26, 27, 28, and 29 had very poor water quality, with a percentage of 4.44% of the total; it was attributed to high levels of sulfate, chloride, calcium, and nitrate. The EWQI results were very consistent with the arithmetic of the WQI: 28.89% in the good water quality category, 22.22% in the poor category, and 2.20% in the extremely poor category, respectively.

Fig.7 illustrates the WQI and EWQI values, which reveal similar results, particularly visible in wells 28 and 29. The FWQI results showed that 60.00% of the wells were classified as having poor water quality, while 15.56% were classified as having average quality and 20.00% fell into the very poor category. This distribution reflects a predominance of poor water quality, consistent with the WQI and EWQI results. It highlights the widespread influence of contaminants such as sulfate, chloride, calcium, and nitrate on groundwater quality in the region.

The correlation matrix in Table 5 highlights the relationship between water quality indices and physicochemical parameters. The arithmetic water quality index (WQI) shows a significant association with key parameters, including EC, TH, Cl-, SO_4^{2-}, Na^+, Ca^{2+}, Mg^{2+}, and NO_3^-. This relationship implies that as the concentrations of important parameters increase, the WQI values also increase, indicating poor water quality. Thus, total hardness (TH) is well correlated with the EWQI, and a moderate correlation is observed between SO_4^{2-}, Ca^{2+} , Mg^{2+} , and NO_3^- with the EWQI. They also have a direct influence on water quality classifications, as they are among the most important parameters in the calculation of the EWQI. However, each is weighted differently according to its relative importance. These physicochemical parameters are assigned a certain weighting coefficient to reflect their impact on the water quality index and allow a better differentiation of risks about groundwater consumption.

The correlation between the fuzzy water quality index (FWQI) and various water quality parameters shows that SO_4^{2-}, Ca^{2+}, and Mg^{2+} have strong negative correlations with the FWQI, indicating a significant impact on water quality. A negative correlation means that as the concentration of these parameters increases, the FWQI decreases, suggesting worse water quality. This reflects the fact that contaminants such as dissolved salts and pollutants tend to lower the FWQI, which is structured to represent better water quality with higher values.

Table 5. Correlation of water quality indices with their physicochemical parameters

Index	pH	EC	Ca^{2+}	Mg^{2+}	HCO_3	Cl^-	SO_4^{2-}	TDS	NO_3^-	Na^+	K^+
WQI	-0.14	**0.54**	**0.77**	**0.71**	0.18	**0.61**	**0.74**	**0.68**	**0.70**	-0.14	0.002
EWQI	-0.08	0.31	**0.50**	0.46	0.18	0.34	0.45	**0.72**	0.39	-0.16	-0.006
FWQI	0.43	-0.27	**-0.63**	**-0.58**	-0.41	-0.36	**-0.73**	-0.32	**-0.50**	-0.003	0.03

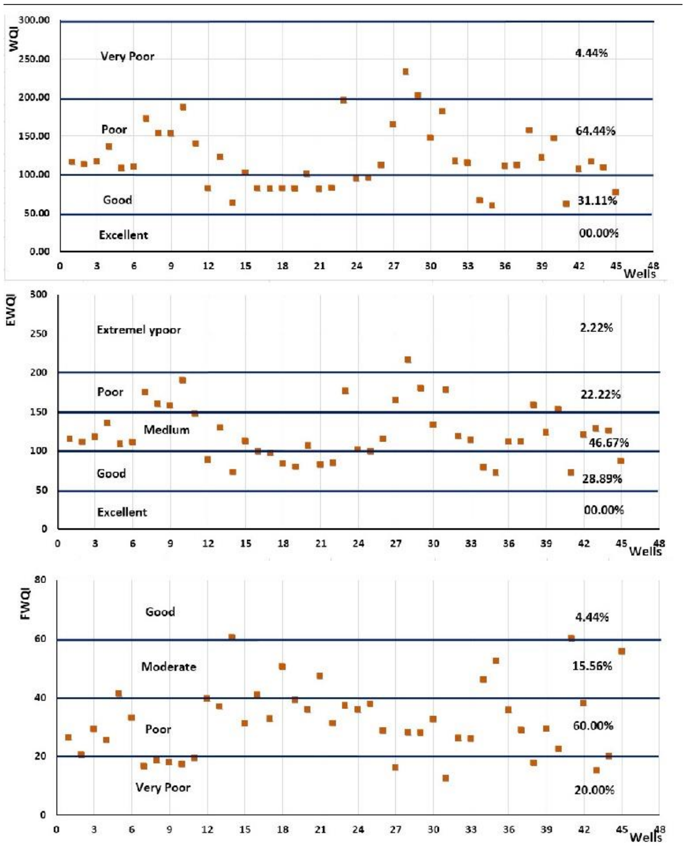

Figure 7. Results of WQI, EWQI, and FWQI for Groundwater Samples

3.9. Spatial Interpolation of Water Quality Indices and Principal Parameters

In Fig.8, the spatial distribution of the values of the proposed quality indices, WQI, EWQI, and Fuzzy FWQI, is presented using the ordinary kriging (OK) method.

To clarify, the prediction of values was performed by applying spatial interpolation techniques (ordinary Kriging and inverse distance weighting, IDW) to estimate groundwater quality at unsampled locations. A subset of the dataset (15% of the total samples) was retained as validation points to assess the accuracy of these methods. Each technique was used to generate predicted values at the validation point locations, which were then compared to the measured values at those points. The root mean square error (RMSE) was calculated as a measure of the difference between the predicted and measured values. By minimizing the RMSE, the method that showed the closest agreement with actual observations was identified as the most reliable for capturing the spatial variability of groundwater quality. This rigorous approach ensures that the predictions are not only mathematically optimized but also scientifically robust to represent spatial patterns [35]-[43]. Ordinary Kriging was preferred because the spherical variogram showed a clear spatial correlation or trend. It considers both the distance and spatial arrangement of data points, providing more accurate predictions for spatially structured data. In contrast, inverse distance weighting (IDW) was less suitable because the variogram showed little spatial correlation, as this method relies only on the distance between points without considering the overall spatial variability.

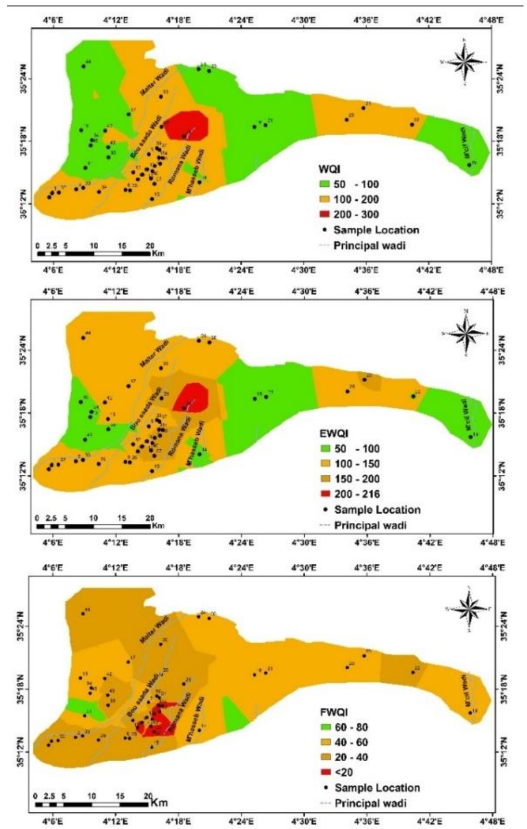

Figure 8. Spatial distribution maps of WQI, EWQI, and FWQI for groundwater samples (by Ordinary Kriging).

These results underscore the significance of advanced models, particularly the Fuzzy Water Quality Index (FWQI) [44], which demonstrates the need for incorporating fuzzy logic into GIS-based groundwater quality assessments. The FWQI model effectively predicts the status of groundwater drinking quality, aligning with practical considerations. It accurately classifies safe groundwater as "high quality" (suitable for direct consumption) and hazardous groundwater as "low quality" (unsuitable for direct use or domestic purposes), thereby enhancing the reliability of groundwater quality evaluations on a broader scale.

Fig.9 illustrates the spatial interpolation of key groundwater quality parameters using the Ordinary Kriging geostatistical method. Elevated concentrations that exceed drinking water standards are primarily concentrated in the Maadher plain, located between the Bousaada and Roumana wadis, and gradually decrease towards the east and west of the plain.

Additionally, high concentrations of chloride (Cl^-) and magnesium (Mg^{2+}) are observed in another area to the east of the study region, also exceeding the drinking water standards. The spatial distribution of electrical conductivity (EC) confirms the presence of two distinct zones with elevated values. Nitrate (NO_3^-) concentrations exceed permissible levels in samples from the Maadher plain and show elevated levels towards the central part of the study area, particularly at the end of wadis.

Spatial distributions of groundwater quality parameters are largely influenced by groundwater flow direction and agricultural activity [45]. The spatial distribution of electrical conductivity (EC) shows the presence of two distinct zones with high values. Nitrate (NO_3^-) concentrations exceed the permissible standard in the Maadher plain samples and show high levels towards the central part of the study area, especially where the wadis end. The spatial distributions of groundwater quality parameters are largely influenced by the direction of groundwater flow and agricultural activity [45].

The high NO_3^- concentrations at the bottom of Bousaada and Roumana wadis highlight the impact of agricultural practices, such as the use of animal and chemical fertilizers, and pollution from local activities found near the wadis. These places are often landfill sites for residents, contributing to groundwater contamination. In our study, we applied ordinary Kriging to the dataset, employing spherical semivariogram models that best fit the data. The kriging approach was chosen to account for spatial correlation, aiming to generate smoother surfaces in regions characterized by poorer water quality. Understanding the variogram curve parameters, such as nugget, threshold, and range, is essential to defining the variogram model, as these parameters indicate the spatial variability influenced by structural and stochastic elements.

The spatial distribution of the three quality indices (WQI, EWQI, and Fuzzy FWQI) yields results that are more similar to each other. According to these maps, the information shows poor quality in the middle part of the study area, more precisely in the agricultural zone of Maadher, at the base of the Bousaada and Roumana hills, particularly at wells 10, 26, 27, 28, 29, and 23. Water quality shows a slight improvement as one moves away from the Maadher plain. Conversely, wells located in the far east and far west of the study area, particularly wells 14, 18, 20, 21, 24, and 25, demonstrate moderate to good water quality. To enhance precision, a comparative analysis of the WQI, EWQI, and FWQI indices was conducted to evaluate their relative performance in predicting groundwater quality in the study area. The results, as depicted in Fig.8, demonstrate that the WQI and EWQI models produce broadly similar outcomes when the same number of quality categories is used.

In contrast, the FWQI values are more distinctly situated between the moderate and poor categories. Notably, the FWQI shows fewer extreme values compared to the WQI and EWQI. The red zone typically indicates groundwater quality parameters with concentrations significantly below their acceptable limits, as outlined by WHO (2011).

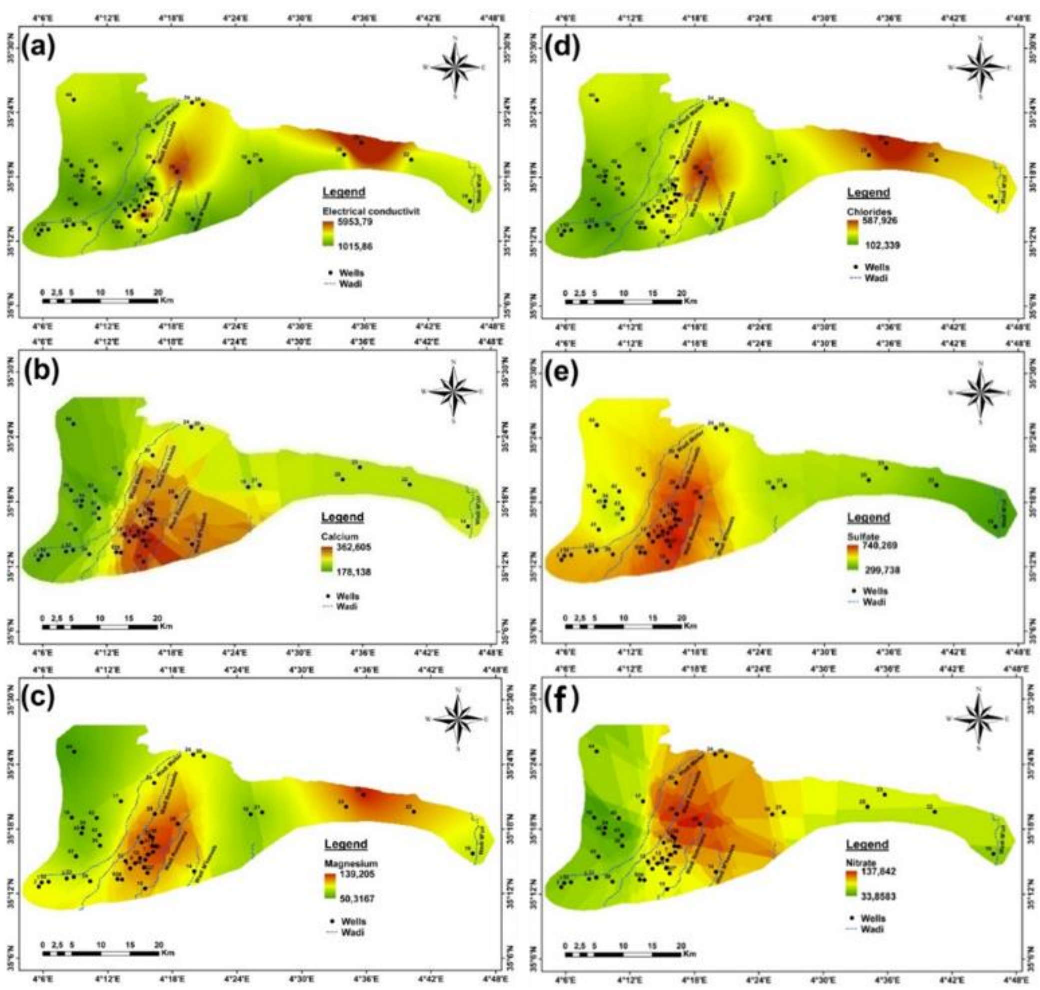

Fig.9. Spatial distribution maps of EC, Ca^{2+}, Mg^{2+}, Cl^-, SO_4^{2-} and NO_3^- using ordinary Kriging

4. Conclusion

The research indicates the impact of anthropogenic activities and overexploitation on groundwater quality in the southern Chott Hodna region, by integrating advanced water quality indices (WQI, EWQI, and fuzzy FWQI) with GIS-based spatial interpolation techniques such as ordinary Kriging, we established a robust framework to assess and monitor groundwater quality effectively. Notably, the fuzzy FWQI model with a triangular membership function based on WHO (2011) demonstrated increased accuracy by reducing extreme classifications, making it a valuable tool for addressing data uncertainties and variability. Spatial analyses identified the Maadher plain as a critical area of groundwater contamination, requiring targeted mitigation efforts. The study identified significant exceedances of WHO standards for key contaminants (SO_4^{2-}, Cl^-, NO_3^- , and Ca^{2+}), highlighting the region's aptness to salinization and pollution. The predominance of sulfate-chloride-calcium-magnesium facies, caused by evaporation and agricultural malpractices, underscores the need for targeted water management strategies to attenuate degradation. Despite these challenges, irrigation indices suggest that in some parts of the region, groundwater remains suitable for agricultural use.

Acknowledgements

The authors thank the Algerian Ministry of Higher Education and Scientific Research for its financial support.

Conflict of interest

The authors declare that there are no conflicts of interest regarding the publication of this manuscript.

Author Contribution Statement

Lakhdar Seraiche and Tahar Selmane contributes to certain figures. Mostafa Dougha was responsible for additional enrichments. Messaoud Ghodbane was responsible for statistical analyses of the data.

References

[1] T. Selmane, M. Dougha, M. Hasbaia, A. Ferhati, and A. Redjem, "Hydrogeochemical processes and multivariate analysis for groundwater quality in the arid Maadher region of Hodna, northern Algeria," *Acta Geochim.*, vol. 41, no. 5, pp. 893-909, 2022, https://doi.org/10.1007/s11631-022-00553-y

[2] J. Kim and K. K. Lee, "Hydrogeochemical signatures for sustainable use of shallow groundwater as a thermal resource at groundwater–surface water mixing zone," *Environ. Earth Sci.*, vol. 81, no. 11, Art. no. 318, 2022,https://doi.org/10.1007/s12665-022-10439-0

[3] H. Belhouchette, E. Boughariou, O. Larayedh, and S. Bouri, "Groundwater quality evaluation and human health risks assessment using the WQI, NPI, and HQnitrate models: case of the Sfax intermediate aquifer, Sahel Tunisia," *Environ. Geochem. Health*, vol. 44, no. 8, pp. 2629-2647, 2022, https://doi.org/10.1007/s10653-021-01053-3

[4] O. El Mountassir, M. Bahir, D. Ouazar, S. Ouhamdouch, A. Chehbouni, and M. Ouarani, "The use of GIS and water quality index to assess groundwater quality of Krimat aquifer, Essaouira, Morocco," *SN Appl. Sci.*, vol. 2, no. 5, pp. 1-16, 2020, https://doi.org/10.1007/s42452-020-2653-z

[5] A. A. Soltani, A. Bermad, H. Boutaghane, A. Oukil, O. Abdalla, M. Hasbaia, and A. Lekir, "An integrated approach for assessing surface water quality: Case of Beni Haroun dam (Northeast Algeria)," *Environ. Monit. Assess.*, vol. 192, no. 10, pp. 1-17, 2020, https://doi.org/10.1007/s10661-020-08572-z

[6] A. Masood, M. Aslam, Q. B. Pham, W. Khan, and S. Masood, "Integrating water quality index, GIS and multivariate statistical techniques towards a better understanding of drinking water quality," *Environ. Sci. Pollut. Res.*, pp. 1-17, 2022, https://doi.org/10.1007/s11356-021-17594-0

[7] E. M. Radouane, A. Chahlaoui, A. Maliki, and A. Boudellah, "Assessment and modeling of groundwater quality by using water quality index (WQI) and GIS technique in Meknes aquifer (Morocco)," *Géol. Ecol. Landscapes*, vol. 7, pp. 126-138, 2021, https://doi.org/10.1080/24749508.2021.1944797.

[8] F. I. Muhammed and None İlker Akmırza, "Assessment of the Water Quality of the Tigris River in the City of Mosul," *Journal of Engineering and Sustainable Development*, vol. 29, no. 5, pp. 664–673, Aug. 2025, doi: https://doi.org/10.31272/jeasd.2903

[9] T. A. Adnan, E. A. Mohammed, and A. S. T. Al-Madhhachi, "Water Quality Index of Tigris River Within Baghdad City, A Review," *Journal of Engineering and Sustainable Development*, vol. 25, no. 3, pp. 34-43, 2021, https://doi.org/10.31272/jeasd.25.3.4.

[10] C. E. Shannon, "A mathematical theory of communication," *Bell Syst. Tech. J.*, vol. 27, no. 3, pp. 379-423, 1948. https://doi.org/10.1002/j.1538-7305.1948.tb01338.x.

[11] Y. Zuanyun, W. Yuanjun, Y. Shaoping, et al., "Comprehensive Evaluation of Geological Environmental Quality and Water Ecological Function in Zipingpu Reservoir Area of Chengdu City," *Water Resour.*, vol. 50, pp. S278–S287, https://doi.org/10.1134/S0097807822602230

[12] I. Khouni, G. Louhichi, and A. Ghrabi, "Use of GIS-based Inverse Distance Weighted interpolation to assess surface water quality: Case of Wadi El Bey, Tunisia," *Environ. Techno. Innov.*, vol. 24, pp. 101-892, 2021, https://doi.org/10.1016/j.eti.2021.101892

[13] N. Saqib, P. K. Rai, S. Kanga, D. Kumar, B. Durin, and S. K. Singh, "Assessment of Ground Water Quality of Lucknow City under GIS Framework Using Water Quality Index (WQI)," *water*, vol. 15, no. 17, Art. no. 3048, 2023, https://doi.org/10.3390/w15173048

[14] A. K. Taloor, R. A. Pir, N. Adimalla, S. Ali, D. S. Manhas, S. Roy, and A. K. Singh, "Spring water quality and discharge assessment in the Basantar watershed of Jammu Himalaya using geographic information system (GIS) and water quality Index (WQI)," *Groundwater Sustain. Dev.*, vol. 10, Art. no. 100364, 2020, https://doi.org/10.1016/j.gsd.2020.100364

[15] B. Boudiaf, I. Dabanli, H. Boutaghane, and Z. Şen, "Temperature and precipitation risk assessment under climate change effect in Northeast Algeria," *Earth Syst. Environ.*, vol. 4, no. 1, pp. 1-14, 2020, https://doi.org/10.1007/s41748-019-00136-7.

[16] S. Chidambaram, M. V. Prasanna, S. Venkatramanan, M. Nepolian, K. Pradeep, B. Panda, et al., "Groundwater quality assessment for irrigation by adopting a new suitability plot and spatial analysis based on fuzzy logic technique," *Environ. Res.*, vol. 204, 2022, Art. no. 111729, https://doi.org/10.1016/j.envres.2021.111729

[17] R. Guiraud, "The main features of the Hodna Chott basin Hydrogeology, Algeria (in French)," *Publi Servi Géol.*, vol. 39, pp. 159–170, 1973.

[18] A. M. Derekov, "Hydrological Studies in the Chott El Hodna basin," *Tech. Rep.*, Food and Agriculture Organization of the United Nations, 1973.

[19] S. Abdesselam, A. Halitim, A. Jan, F. Trolard, and G. Bourrié, "Anthropogenic contamination of groundwater with nitrate in arid regions: case study of southern Hodna (Algeria)," *Environ. Earth Sci.*, vol. 70, no. 5, pp. 2129-2141, 2013, https://doi.org/10.1007/s12665-012-1834-5

[20] ANRH (Agence Nationale des Ressources Hydrauliques), "Modeling of the Hodna aquifer. Mission I: data collection, analysis, and synthesis (in French)," *Tech. Rep.*, Algeria, 2006.

[21] F. Wilde, "Water-quality sampling by the US Geological Survey: standard protocols and procedures," *US Géol. Surv. Fact Sheet*, vol. 312, pp. 2, 2010, https://doi.org/10.3133/fs20103121

[22] E. Sener, S. Sener, and S. Varol, "Appraisal of groundwater quality with WQI and human health risk assessment in Karamik wetland and surroundings (Afyonkarahisar/Turkey)," *Environ. Geochem. Health*, vol. 45, pp. 1499-1523, 2022, https://doi.org/10.1007/s10653-022-01282-0

[23] F. I. Oseke, G. K., Anornu, K. A., Adjei, and M. O. Eduvie, "Assessment of water quality using GIS techniques and water quality index in reservoirs affected by water diversion," *Water-Energy Nexus*, vol. 4, pp. 25-34, 2021, https://doi.org/10.1016/j.wen.2020.12.002

[24] World Health Organization (WHO), "Guidelines for drinking-water quality," 2011. [Online]. Available: http://www.who.int/water_sanitation_health/publications/2011/dwq_guidelines/en/.

[25] A. Ram, S. K. Tiwari, H. K. Pandey, A. K. Chaurasia, S. Singh, and Y. V. Singh, "Groundwater quality assessment using water quality index (WQI) under GIS framework," *Appl. Water Sci.*, vol. 11, pp. 1-20, 2021, https://doi.org/10.1007/s13201-021-01376-7

[26] C. R. Ramakrishnaiah, C. Sadashivaiah, and G. Ranganna, "Assessment of water quality index for the groundwater in Tumkur Taluk, Karnataka State, India," *E-J. Chem.*, vol. 6, no. 2, pp. 523-530, 2009, https://doi.org/10.1155/2009/757424

[27] P.-Y. Li, H. Qin, and J.-H. Wu, "Groundwater quality assessment based on improved water quality index in Pengyang County, Ningxia, Northwest China," *J. Chem.*, vol. 7, suppl. 1, pp. S209-S216, 2010, https://doi.org/10.1155/2010/451304

[28] P. Singh and P. Verma, "A Comparative Study of Spatial Interpolation Technique (IDW and Kriging) for Determining Ground Water Quality," in *GIS Geostatistical Techniques Groundwater Sci.*, India; 2019, ch 5, pp. 43-56, https://doi.org/10.1016/B978-0-12-815413-7.00005-5

[29] M. K. Jha et al., "Assessing groundwater quality for drinking water supply using hybrid fuzzy-GIS-based water quality index," *Water Res.*, vol. 179, art. no. 115867, 2020, https://doi.org/10.1016/j.watres.2020.115867

[30] J. O. Oladipo, A. S. Akinwumiju, O. S. Aboyeji, and A. A. Adelodun, "Comparison between fuzzy logic and water quality index methods: a case of water quality assessment in Ikare community, Southwestern Nigeria," *Environ. Challenges*, vol. 3, art. no. 100038, 2021, https://doi.org/10.1016/j.envc.2021.100038

[31] O. Dhaoui, B. Agoubi, I. M. Antunes, L. Tlig, and A. Kharroubi, "Groundwater quality for irrigation in an arid region—application of fuzzy logic," Environmental Science and Pollution Research, vol. 30, no. 11, pp. 29773–29789, Nov. 2022, https://doi.org/10.1007/s11356-022-24334-5

[32] Shwetank, Suhas, and J. K. Chaudhary, “Estimation of groundwater contamination using fuzzy logic: A case study of Haridwar, India,” Groundwater for Sustainable Development, vol. 8, pp. 644–653, Apr. 2019, https://doi.org/10.1016/j.gsd.2019.03.004

[33] D. R. Pathak and N. P. Bhandary, “Evaluation of groundwater vulnerability to nitrate in shallow aquifer using multi-layer fuzzy inference system within GIS environment,” Groundwater for Sustainable Development, vol. 11, p. 100470, Oct. 2020, https://doi.org/10.1016/j.gsd.2020.100470

[34] D. Chapman, *Water Quality Assessments: A Guide to the Use of Biota, Sediments, and Water in Environmental Monitoring*, CRC Press, 2021. https://doi.org/10.1201/9781003062103

[35] Q. Yang, Z. Li, C. Xie, J. Liang, and H. Ma, "Risk assessment of groundwater hydrochemistry for irrigation suitability in Ordos Basin, China," *Nat. Hazards*, vol. 101, pp. 309-325, 2020, https://doi.org/10.1007/s11069-018-3451-4

[36] E. O. Thomas, "Spatial evaluation of groundwater quality using factor analysis and geostatistical Kriging algorithm: a case study of Ibadan Metropolis, Nigeria," *Water Pract. Technol.*, vol. 18, no. 3, pp. 592-607, 2023, https://doi.org/10.2166/wpt.2023.023

[37] M. G. Uddin, A. I. Olbert, and S. Nash, "Assessment of water quality using Water Quality Index (WQI)," *Ecol. Indic.*, vol. 85, pp. 966-982, 2020. [Online]. Available: http://hdl.handle.net/10379/16427

[38] A. A. Rostami, V. Karimi, R. Khatibi, and B. Pradhan, "An investigation into seasonal variations of groundwater nitrate by spatial modeling strategies at two levels by kriging and co-kriging models," *J. Environ. Manage.*, vol. 270, art. no. 110843, 2020, https://doi.org/10.1016/j.jenvman.2020.110843

[39] C. Munyati and N. I. Sinthumule, "Comparative suitability of ordinary kriging and Inverse Distance Weighted interpolation for indicating intactness gradients on threatened savannah woodland and forest stands," *Environ. Sustain. Indic.*, vol. 12, art. no. 100151, 2021, https://doi.org/10.1016/j.indic.2021.100151

[40] C. W. Fetter, *Applied Hydrogeology*, 4th ed., Waveland Press, USA, 2018, 559 p.

[41] R. J. Gibbs, "Mechanisms controlling world water chemistry," *Science*, vol. 170, no. 3962, pp. 1088-1090, 1970, https://doi.org/10.1126/science.170.3962.1088.

[42] X. Wang, C. Xiao, W. Yang, X. Liang, L. Zhang, and J. Zhang, "Analysis of the quality, source identification and apportionment of the groundwater in a typical arid and semi-arid region," *J. Hydrol.*, vol. 625, art. no. 130169, 2023, https://doi.org/10.1016/j.jhydrol.2023.130169

[43] K. Masroor, F. Fanaei, S. Yousefi, M. Raeesi, H. Abbaslou, A. Shahsavani, and M. Hadei, "Spatial modelling of PM2.5 concentrations in Tehran using Kriging and inverse distance weighting (IDW) methods," *J. Air Pollut. Health*, vol. 5, no. 2, pp. 89-96, 2020, https://doi.org/10.18502/japh.v5i2.4237

[44] G. Ellina, G. Papaschinopoulos, and B. K. Papadopoulos, "Research of fuzzy implications via fuzzy linear regression in data analysis for a fuzzy model," *J. Comput. Methods Sci. Eng.*, vol. 20, no. 3, pp. 879-888, 2020, https://doi.org/10.3233/JCM-194015

[45] M. Dougha and M. Hasbaia, "Contribution of the multivariate analysis and origin for groundwater quality of mixed aquifer in the M’sila plain (Algeria)," *Int. J. Hydrol. Sci. Technol.*, vol. 9, no. 2, pp. 154–172, 2019, https://doi.org/10.1504/IJHST.2019.098160